

## Multi-scale synthetic aperture radar remote sensing for archaeological prospection in Han Hangu Pass, Xin'an China

Fulong Chen<sup>a,b</sup>, Aihui Jiang<sup>c,a</sup>, Panpan Tang<sup>a,b</sup>, Ruixia Yang<sup>a,b</sup>, Wei Zhou<sup>a,b</sup>, Hongchao Wang<sup>d</sup>, Xin Lu<sup>d</sup> and Timo Balz<sup>e</sup>

<sup>a</sup>Key Laboratory of Digital Earth Science, Institute of Remote Sensing and Digital Earth, Chinese Academy of Sciences, Beijing, China; <sup>b</sup>International Centre on Space Technologies for Natural and Cultural Heritage under the Auspices of UNESCO, Beijing, China; <sup>c</sup>College of Geodesy and Geomatics, Shandong University of Science and Technology, Qingdao, China; <sup>d</sup>Institute of conservation and management of Xin'an Hangu Pass (Han Dynasty), Cultural relic bureau of Xin'an County, Luoyang, China; <sup>e</sup>State Key Laboratory of Information Engineering in Surveying, Mapping and Remote Sensing, Wuhan University, Wuhan, China

### ABSTRACT

Increasing availability of multi-resolution synthetic aperture radar (SAR) data enabled us to demonstrate the benefits of the existing imaging solutions offered by radar satellites for purposes of archaeological prospection. In this study, mid-resolution L-band phased array type L-band synthetic aperture radar (PALSAR) to high-to-very-high-resolution X-band TerraSAR-X/TanDEM-X TerraSAR-X add-on for digital elevation measurements (TanDEM-X) (Stripmap/Staring Spotlight) images were synergistically applied for the archaeological prospection at the Han Hangu Pass, in Xin'an, China. First, the evidence and the stretching direction of the outer walls of the pass were identified from the temporal-averaged products of PALSAR and the terrain from TanDEM Co-registered Single-Look Data. Then, the spatial layout of archaeological monuments (previously documented as well as recently discovered) was observed in the visualization-enhanced Staring Spotlight TerraSAR-X imagery owing to its high spatial and radiometric resolution. The findings of this study highlight the effectiveness of using integrated multi-scale SAR remote sensing data from different platforms in archaeology.

### ARTICLE HISTORY

Received 29 June 2016

Accepted 7 September 2016

## 1. Introduction

Archaeological remains are not renewable resource for providing information (Lasaponara et al. 2016) that is beneficial for the understanding of past human civilizations. Remote sensing, particularly the high-resolution optical approaches, has been an important tool in archaeological prospection using the established archaeological shadow, crop, soil and damp marks (Lasaponara and Masini 2011; Agapiou et al. 2013; Agapiou and Lysandrou 2015). Recently, the potential of radar remote sensing in archaeology has been of increasingly interest to the geoarchaeology community (Garrison et al. 2011; Dore et al. 2013; Lasaponara and Masini 2013; Linck et al. 2013; Conesa et al. 2014; Erasmi et al. 2014; Chen et al. 2015a). Compared with optical approaches, synthetic aperture radar (SAR) is

**CONTACT** Fulong Chen  [chenfl@radi.ac.cn](mailto:chenfl@radi.ac.cn)  Key Laboratory of Digital Earth Science, Institute of Remote Sensing and Digital Earth, Chinese Academy of Sciences, Beijing, China

© 2016 Informa UK Limited, trading as Taylor & Francis Group

distinguished by its all-weather, all-day operational capabilities as well as interferometry and polarimetry outcomes that significantly facilitate data analyses and interpretation (Chen, Lasaponara, and Masini 2015b). The occurrence of multi-source space-borne SAR from either the first-generation (e.g., Seasat and Envisat advanced synthetic aperture radar (ASAR) or second-generation (e.g., TerraSAR/TanDEM-X and advanced land observing satellite (ALOS) phased array type L-band synthetic aperture radar (PALSAR)-2) sensors provide abundance of multi-temporal, high-resolution and polarimetric archival data that are beneficial for performance assessment (Chen et al. 2016) and integrated analysis of SAR images in archaeology. Apart from optical approaches (Crawford 1929; Rowlands and Sarris 2007; Agapiou, Alexakis, and Hadjimitsis 2014; Keay, Parcak, and Strutt 2014), SAR applications in archaeology were increasingly concerned by teamwork between archaeologists and remote sensing experts (Tapete and Cigna forthcoming), bringing into a golden era (Chen, Lasaponara, and Masini 2015b) along with the occurrence of second-generation space-borne SAR platforms. Agapiou and Lysandrou (2015) reported that 'radar images' are among top-used terms in relevant remote sensing literatures between 2013 and 2015 (Tapete and Cigna forthcoming). Challenges of SAR applications in archaeology, such as the complexity of data processing and difficulties associated with results interpretation, are progressively overcome contributed by the increasing number of literatures coupled with the enhanced collaboration between different professionals. Earlier satellite data sets with medium resolution (e.g., Envisat ASAR and ALOS PALSAR-1) provide long archives of images to perform the landscape archaeology as well as time series analyses (Cigna et al. 2013; Stewart, Lasaponara, and Schiavon 2014); however, their capability in the detection and monitoring of monuments is still limited. Generally, integrated investigations combining large-scale landscape and local-scale monuments would provide comprehensive results. Based on our earlier, pilot studies (Chen et al. 2015a; Chen, Lasaponara, and Masini 2015b, 2016), we demonstrated the benefits of the existing SAR imaging solutions for purposes of archaeological prospection in the Han Hangu Pass, Xin'an County, Henan Province, China, using multi-resolution data. We combined the use of mid-resolution ALOS PALSAR data and high-resolution TerraSAR/TanDEM-X data for the landscape scale with the very high-resolution (VHR) Staring Spotlight TerraSAR-X data for the monument-scale; the results, as reported in the following sections, are quite promising for the future applications of such integrated, multi-scale and multi-data approaches to archaeological prospection.

## 2. Study site and data

### 2.1. Han Hangu Pass

Han Hangu Pass was originally built in 3rd year of the Yuanding period of Han Emperor Wudi (around 114 BC). It was the first easternmost pass from the central plains of China leading into the land-based Silk Road of those times. The relics of this pass have been included into the cluster of Silk Road sites: the Routes Network of Chang'an-Tianshan Corridor that was inscribed on the UNESCO World Heritage List in 2014. The gate of Han Hangu Pass faces Jian River in the east (Xin'an County to the west, Fenghuang Mountain to the north and Qinglong Mountain to the south, respectively; see Figure 1). As one of the eight important gates for the capital city of Luoyang of Han-Tang dynasty (2000 ~ 900 BP), the defence system of the gate was rather complex. One prevailing

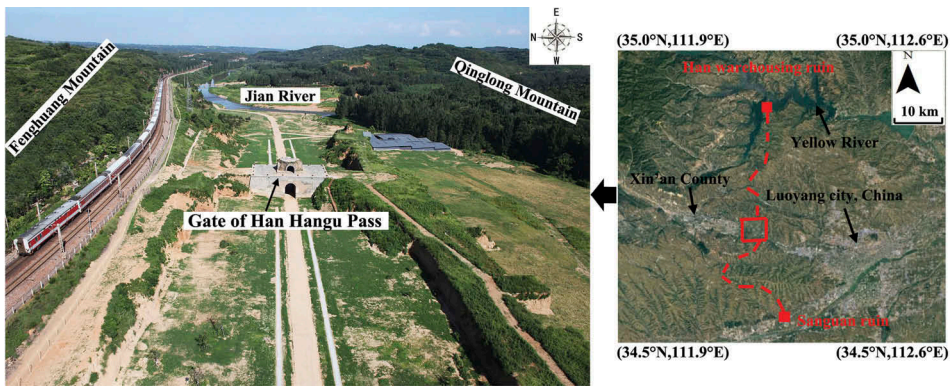


**Figure 1.** Landscape and location of Han Hangu Pass. The barrier system of the pass comprises the gate (marked by the red rectangle) and outer defending walls (marked by red-dotted lines) extending north to the Han warehousing ruin (highlighted by a red-square point) and south to the Sanguan ruin (highlighted by another red-square point), as overlapped on the Google Earth imagery.

hypothesis (Wang et al. 2014) postulates that the defending walls are extended, connecting the gate to the Han warehousing Ruin (in the vicinity of Yellow River) in the north and to the Sanguan Ruin in the south (marked by the red dotted line in Figure 1). Moreover, earlier archaeological field surveys have implied that the Pass was complemented by an ancient county city (Wang et al. 2014), but supporting evidence for this hypothesis, for example, the spatial layout the city wall and its foundations, is lacking.

## 2.2. SAR data

Multisource space-borne Single Look Complex SAR data, including L-band ALOS PALSAR and X-band TerraSAR/TanDEM, were collected for the archaeological prospection in Xi'an Han Hangu Pass. Totally, 20 scenes of ascending mid-resolution PALSAR data were acquired for the period from 3 January 2007 to 1 March 2011. Among those revisit cycle data, 9 scenes were in Fine Beam Single (FBS) polarization with horizontal transmit and horizontal receive (HH) polarization and the other 11 were in Fine Beam Dual (FBD) polarization with horizontal transmit and horizontal receive/horizontal transmit and vertical receive dual polarization. The ground resolutions of PALSAR FBS and FBD images are approximately 8 and 16 m, respectively, given an incidence angle of 34.3°. The Stripmap bistatic TanDEM Co-registered Single Look Slant range Complex (CoSSC) data (with a ground resolution of 3 m and an incidence angle of 37°) were acquired on 8 January 2014 for digital elevation model (DEM) generation and terrain analysis. For the VHR, one scene of Staring Spotlight Single Look Slant range Complex (SSC) TerraSAR-X, ascending imagery with a ground-range resolution of 0.9 m and an incidence angle of 40.8°, was acquired on 6 May 2016.

## 3. Solution of the coarse-fine observation

Mid-resolution SAR data for the landscape scale (Tapete et al. 2013) and VHR for the monument scale (Tapete, Cigna, and Donoghue 2016) were integrated in this study to

test the use of multi-resolution data for a comprehensive study of the Han Hangu Pass. In this article, we demonstrated benefits of the existing SAR imaging solutions based on previous work (Chen et al. 2015a; Chen, Lasaponara, and Masini 2015b, 2016) conducted by the same research group as well as more new refinements and improvements that were developed, such as (i) the multi-scale imaging from the landscape to monuments and (ii) the detection of relief-linked traces using InSAR-derived DEM, during the course of this study.

Radiometric calibration was first applied to the L-band FBS/FBD PALSAR and X-band Staring Spotlight TerraSAR data to obtain the radar backscattering coefficients. Furthermore, the multi-temporal PALSAR data (revisit-cycle acquisitions) were co-registered with an accuracy of up to 1/8 pixels in the preprocessing step.

For the landscape-scale analysis, stacked mid-resolution PALSAR data were first applied for temporal averaging. Range spacing of FBD images with HH polarization were over-sampled with a factor of two, which is a mandatory step prior to the co-registration into a reference imagery of FBS with HH polarization. The temporal-averaged imagery allows the reduction of speckle noise, enhancing the temporally correlated signals linked to the physical properties of the observed archaeological features. Generally, the effective number of looks (ENL) of imagery produced by averaging  $n$  SAR images could be increased by a factor of  $\sqrt{n}$ . For each image pixel  $i$ , the average backscattering coefficient  $\bar{\sigma}_i^0$  can be calculated by the following formula (Chen et al. 2016):

$$\bar{\sigma}_i^0 = \frac{1}{n} \sum_{t=t_0}^{t=t_n} \sigma_i^0(t) \quad (1)$$

where  $t_0$  and  $t_n$  are the times of acquisition of the first and last PALSAR scene,  $n$  is the total number of scenes composing the stack and  $\sigma_i^0(t)$  is the radar backscattering coefficient of the pixel at the time  $t$ . Then, the Stripmap bistatic TanDEM CoSSC images were applied for building the DEM (an essential data source for the identification of relief-linked archaeological traces) using a complete radar interferometry procedure including baseline estimation, interferogram generation, adaptive filter and coherence generation, phase unwrapping, re flattening, phase to height conversion and geocoding. Height values of the scenario were then calculated using interferometric phases and the parameters of radar imaging:

$$h = -\frac{\varphi \lambda R \sin \theta}{4\pi B_{\perp}} \quad (2)$$

where  $h$  is the estimated height;  $\varphi$  is unwrapped phase,  $\lambda$  is wavelength of radar signal,  $R$  is slant distance between sensor and observed feature,  $\theta$  is incidence angle and  $B_{\perp}$  normal baseline, respectively. For the WorldDEM products from TanDEM CoSSC data, a high resolution terrain information (HRTI)-3 specification (absolute horizontal accuracy <12 m, relative vertical accuracy <2 m) can be attained (AIRBUS 2016). In this study, the accuracy of derived DEM was a bit worse than the HRTI-3 specification due to the fact that only one image pair was processed.

The VHR resolution Staring Spotlight TerraSAR imagery, with a spatial resolution better than 1 m, was used for the identification of archaeological features at the

monument scale. In general, high-resolution and/or VHR SAR data are sensitive to the micro-relief features (Chen et al. 2015a; Tapete and Cigna [forthcoming](#)) of archaeological remains. This is an advantage of SAR remote sensing over optical imagery-based approaches where spectral dispersion between the archaeological remains and their surroundings could be poorly defined. Past investigations (Chen et al. 2015a) indicated that a single-date high-resolution/VHR amplitude SAR imagery could provide a cost-effective tool to detect archaeological features accompanied with physical anomalies of crop, soil and damp, micro-relief marks.

#### 4. Results and interpretations

As described in [Section 3](#), the multi-scale imaging solution with sub-procedures of stacking averaging, CoSSC interferometric processing and imagery enhancement, was applied for the archaeological prospection in Han Hangu Pass.

Intense *in-situ* archaeological surveys (with a spatial coverage of 140,000 m<sup>2</sup>) were conducted in Han Hangu Pass during 2012–2013. These studies allowed us to understand the spatial layout and the depth superposition of monuments in the site. For example, we were able to discern locations where the defending wall was damaged or vulnerable to damage caused by the combination of natural erosion and anthropogenic activities (e.g., civil wars and cultivations) in past 2000 years, as marked by black lines in [Figure 2\(a\)](#).

In this study, the 1 × 3 multi-look operator was applied for the co-registered PALSAR data, resulting in the amplitude image stack with a ground resolution of 8 m. About 20 scenes of PALSAR data were stacked to obtain the temporal-averaged imagery, as illustrated in [Figure 2\(b\)](#). It was clear that the temporally uncorrelated speckle noise has been mitigated due to the enhancement of the ENL. Note that the outer defending walls identified by the field surveys in 2012–2013 ([Figure 2\(a\)](#)) were not visible in the stacked PALSAR imagery constrained by the complicated local topography. However, a new section of suspected defending walls in the north were identified by the linear backscattering anomaly on the temporal-averaged imagery (see dotted red lines in [Figure 2\(b\)](#)). This anomaly was caused by the combination of the preserved trace in conjunction with the physical property of the consolidated rammed earth link to the ancient walls. Furthermore, the relief-linked signature from archaeological features can be magnified in the case of a parallel direction between SAR flights and the stretching of the linear geoglyph, resulting in the discrimination of defending walls on the stacked PALSAR imagery with spatial resolution of 8 m. Those newly detected defending walls are generally buried with a depth of 0.5–1 m, verified by the wall ruins identified in the 2012–2013 field surveys ([Figure 2\(a\)](#)). *In-situ* evidences of linear traces were also observed in the field visit in June 2016. Afterwards, the terrain analysis was implemented using the TanDEM CoSSC-derived DEM ([Figure 2\(c\)](#)). It is interesting that the trend of outer walls in the north is consistent with the ridge direction interpreted by the terrain barrier in optimization the defending performance. The direction of outer walls in the south can also be determined, as highlighted by the dotted red lines in [Figure 2\(c\)](#). Nevertheless, their precise locations are still unknown due to the lack of *in-situ* evidence and/or evidence supported by the interpretation of PALSAR images.

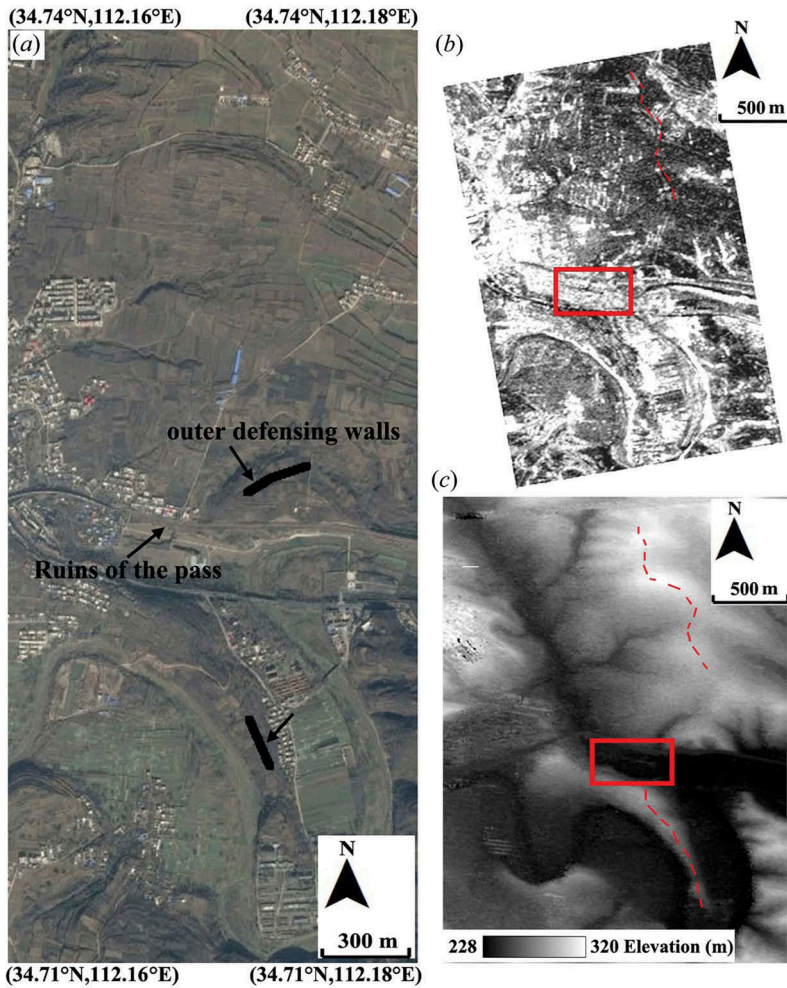


**Figure 2.** Identification of outer defending walls combined temporal-averaged PALSAR with DEM data of TanDEM CoSSC. (a) Outer defending walls detected in past archaeological surveys and marked as black lines overlapped with Google Earth imagery, (b) the north stretching walls identified by temporal-averaged PALSAR imagery and marked as dotted red line and (c) the location of the south stretching walls interpreted from the DEM data of the TanDEM CoSSC image pair, and marked by the dotted red line. The core region of Han Hangu Pass is the red rectangle in Figures 2(b), (c), respectively.

For the detection of local-scale monuments (see Figure 3), the Staring Spotlight SSC TerraSAR imagery was used. The amplitude of TerraSAR-X imagery was firstly geocoded using control points with the World geodetic system 1984 coordinates, followed by an enhanced Lee speckle filter (Lopes, Touzi, and Nezry 1990) in conjunction with the logarithmic-stretching enhancement. Owing to the VHR, the spatial layout of important monuments known (e.g., Jiming tower and Wangqi tower) as well as the trace of excavations in the site (marked by the yellow subzone '1' in Figure 3(a)) can be observed. The presence of 'Inner north wall' and 'Inner south wall' is more sharpened on SAR imagery (Figure 3(b)) owing to its sensitivity of micro-reliefs. Historical

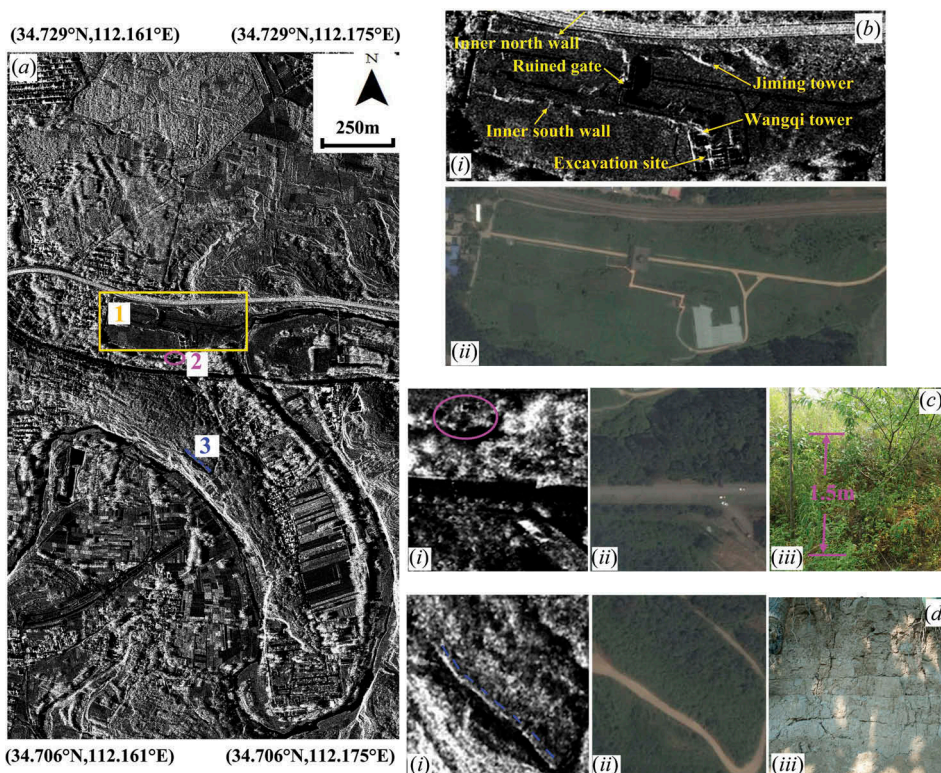


**Figure 3.** Identification of monuments by VHR Staring Spotlight TerraSAR imagery. (a) Synoptic chart of Han Hangu Pass with hotspots and archaeological features highlighted by '1, 2 and 3'; (b) subzone of '1' on TerraSAR imagery (i) with important monuments known, such as Jiming tower and Wangqi tower, in the core archaeological area and on Google Earth imagery (ii); (c) purple circle of '2' indicating a beacon-tower ruin on TerraSAR imagery (i), Google Earth imagery (ii) and a photograph with a regular and raised mild-terrace (a height of 1.5 m) (iii); (d) dotted blue line of '3' on TerraSAR imagery (i) indicating the outer wall in the south, Google Earth imagery (ii) and a photograph with the trace of rammed earth walls (iii). Photos in Figure 3(c), (d) were obtained during the field visit in June 2016.

documents indicate that a beacon tower (element of the gate's defending system) was located at the north foot of the Qinglong Mountain. This ruin was existed before the construction of the Highway G310 in 2008. A hotspot with the radius of 60 m was determined using information from historical records as well as the face-to-face survey to local residents. Then, this area was imaged by the VHR TerraSAR-X and Google Earth (Image @ 2016 DigitalGlobe) optical imagery (Figure 3(c)). The beacon tower ruin (marked by the purple circle '2' in Figure 3(a)) was identified on SAR imagery using the shadow mark and the regular topology (Chen et al. 2015a) versus the regular shape observed only on the latter. The field visit (June 2016) pointed this ruin to a regular and raised mild-terrace (a height of 1.5 m) with shrubs (Figure 3(c)). Moreover, although not visible in the optical imagery of Google Earth (Image @ 2016 DigitalGlobe), the trace of southern outer walls (marked by the blue dotted line '3' in Figure 3(a)) was detected by the dihedral backscattering of the linear remain on SAR imagery (Figure 3(d)), which was

further verified by the presence of the rammed earth wall, as shown by the field photo obtained in June 2016.

## 5. Conclusion

In this article, the potential and feasibility of multi-scale SAR remote sensing in archaeological prospection was assessed in the Han Hangu Pass site and its surrounding landscape using mid-high to VHR L-band PALSAR and X-band TerraSAR/TanDEM data. The experimental results based on the multi-scale imaging solution indicated that (i) the combination of temporal-averaged SAR imagery with the InSAR-derived DEM is effective for landscape-scale archaeology; it allowed the identification of the north-stretching walls by the newly discovered linear anomalies as well as the location of the south-stretching walls by the terrain analysis in defensing. (ii)VHR SAR data (spatial resolution <1 m) provides an essential tool in detecting local-scale monuments in archaeological sites (e.g., south-trending walls and the beacon-tower ruin) by taking advantage of the anomalies of relief-topology, particularly when the spectral discrimination between archaeological remains and the surroundings is not sharp as in the case of many optical images for the detection of rammed earth walls (prevailing architectures in ancient China dating back to 2000 years).

## Disclosure statement

No potential conflict of interest was reported by the authors.

## Funding

This research was supported by funding from Hundred Talents Program of the Chinese Academy of Sciences (CAS) (Y5YR0300QM) and Youth Director Fund Category-A of Institute of Remote Sensing and Digital Earth, CAS.

## References

- Agapiou, A., D. D. Alexakis, and D. G. Hadjimitsis. 2014. "Spectral Sensitivity of ALOS, ASTER, IKONOS, LANDSAT and SPOT Satellite Imagery Intended for the Detection of Archaeological Crop Marks." *International Journal of Digital Earth* 7: 351–372. doi:10.1080/17538947.2012.674159.
- Agapiou, A., D. G. Hadjimitsis, A. Sarris, A. Georgopoulos, and D. D. Alexakis. 2013. "Optimum Temporal and Spectral Window for Monitoring Crop Marks over Archaeological Remains in the Mediterranean Region." *Journal of Archaeological Science* 40: 1479–1492. doi:10.1016/j.jas.2012.10.036.
- Agapiou, A., and V. Lysandrou. 2015. "Remote Sensing Archaeology: Tracking and Mapping Evolution in European Scientific Literature from 1999 to 2015." *Journal of Archaeological Science: Reports* 4: 192–200. doi:10.1016/j.jasrep.2015.09.010.
- AIRBUS. "WorldDEM™, The New Standard of Global Elevation Models. Accessed 6 June 2016. <http://www.intelligence-airbusds.com/worlddem>.
- Chen, F., R. Lasaponara, and N. Masini. 2015b. "An Overview of Satellite Synthetic Aperture Radar Remote Sensing in Archaeology: From Site Detection to Monitoring." *Journal of Cultural Heritage*. doi:10.1016/j.culher.2015.05.003.

- Chen, F., N. Masini, J. Liu, J. You, and R. Lasaponara. 2016. "Multi-Frequency Satellite Radar Imaging of Cultural Heritage: The Case Studies of the Yumen Frontier Pass and Niya Ruins in the Western Regions of the Silk Road Corridor." *International Journal of Digital Earth* 1–18. doi:[10.1080/17538947.2016.1181213](https://doi.org/10.1080/17538947.2016.1181213).
- Chen, F., N. Masini, R. Yang, P. Milillo, D. Feng, and R. Lasaponara. 2015a. "A Space View Of Radar Archaeological Marks: First Applications of COSMO-SkyMed X-Band Data." *Remote Sensing* 7: 24–50. doi:[10.3390/rs70100024](https://doi.org/10.3390/rs70100024).
- Cigna, F., D. Tapete, R. Lasaponara, and N. Masini. 2013. "Amplitude Change Detection with ENVISAT ASAR to Image the Cultural Landscape of the Nasca Region, Peru." *Archaeological Prospection* 20: 117–131. doi:[10.1002/arp.v20.2](https://doi.org/10.1002/arp.v20.2).
- Conesa, F. C., N. Devan  ry, A. L. Balbo, M. Madella, and O. Monserrat. 2014. "Use of Satellite sar for Understanding Long-Term Human Occupation Dynamics in the Monsoonal Semi-Arid Plains of North Gujarat, India." *Remote Sensing* 6: 11420–11443. doi:[10.3390/rs6111420](https://doi.org/10.3390/rs6111420).
- Crawford, O. G. S. 1929. "Air Photography for Archaeologists." *Ordnance Survey Professional Papers, new series*, 12. Southampton: HMSO.
- Dore, N., J. Patruno, E. Pottier, and M. Crespi. 2013. "New Research in Polarimetric SAR Technique for Archaeological Purposes Using ALOS PALSAR Data." *Archaeological Prospection* 20: 79–87. doi:[10.1002/arp.v20.2](https://doi.org/10.1002/arp.v20.2).
- Erasmı, S., R. Rosenbauer, R. Buchbach, T. Busche, and S. Rutishauser. 2014. "Evaluating the Quality and Accuracy of TanDEM-X Digital Elevation Models at Archaeological Sites in the Cilician Plain, Turkey." *Remote Sensing* 6: 9475–9493. doi:[10.3390/rs6109475](https://doi.org/10.3390/rs6109475).
- Garrison, T. G., B. Chapman, S. Houston, E. Roman, and J. L. G. Lopez. 2011. "Discovering Ancient Maya Settlements Using Airborne Radar Elevation Data." *Journal of Archaeological Science* 38: 1655–1662. doi:[10.1016/j.jas.2011.02.031](https://doi.org/10.1016/j.jas.2011.02.031).
- Keay, S. J., S. H. Parcak, and K. D. Strutt. 2014. "High Resolution Space and Ground-Based Remote Sensing and Implications for Landscape Archaeology: The Case from Portus, Italy." *Journal of Archaeological Science* 52: 277–292. doi:[10.1016/j.jas.2014.08.010](https://doi.org/10.1016/j.jas.2014.08.010).
- Lasaponara, R., G. Leucci, N. Masini, R. Persico, and G. Scardozzi. 2016. "Towards an Operative Use of Remote Sensing for Exploring the Past Using Satellite Data: The Case Study of Hierapolis (Turkey)." *Remote Sensing of Environment* 174: 148–164. doi:[10.1016/j.rse.2015.12.016](https://doi.org/10.1016/j.rse.2015.12.016).
- Lasaponara, R., and N. Masini. 2011. "Satellite Remote Sensing in Archaeology: Past, Present and Future Perspectives." *Journal of Archaeological Science* 38: 1995–2002. doi:[10.1016/j.jas.2011.02.002](https://doi.org/10.1016/j.jas.2011.02.002).
- Lasaponara, R., and N. Masini. 2013. "Satellite Synthetic Aperture Radar in Archaeology and Cultural Landscape: An Overview." *Archaeological Prospection* 20: 71–78. doi:[10.1002/arp.v20.2](https://doi.org/10.1002/arp.v20.2).
- Linck, R., T. Busche, S. Buckreuss, J. W. E. Fassbinder, and S. Seren. 2013. "Possibilities of Archaeological Prospection by High-Resolution X-Band Satellite Radar-A Case Study from Syria." *Archaeological Prospection* 20: 97–108. doi:[10.1002/arp.v20.2](https://doi.org/10.1002/arp.v20.2).
- Lopes, A., R. Touzi, and E. Nezry. 1990. "Adaptive Speckle Filters and Scene Heterogeneity." *IEEE Transactions on Geoscience and Remote Sensing* 28: 992–1000. doi:[10.1109/36.62623](https://doi.org/10.1109/36.62623).
- Rowlands, A., and A. Sarris. 2007. "Detection of Exposed and Subsurface Archaeological Remains Using Multi-Sensor Remote Sensing." *Journal of Archaeological Science* 34: 795–803. doi:[10.1016/j.jas.2006.06.018](https://doi.org/10.1016/j.jas.2006.06.018).
- Stewart, C., R. Lasaponara, and G. Schiavon. 2014. "Multi-Frequency, Polarimetric SAR Analysis for Archaeological Prospection." *International Journal of Applied Earth Observation and Geoinformation* 28: 211–219. doi:[10.1016/j.jag.2013.11.007](https://doi.org/10.1016/j.jag.2013.11.007).
- Tapete, D., and F. Cigna. Forthcoming. "Trends and Perspectives of Space-Borne SAR Remote Sensing for Archaeological Landscape and Cultural Heritage Applications." *Journal of Archaeological Science: Reports* doi:[10.1016/j.jasrep.2016.07.017](https://doi.org/10.1016/j.jasrep.2016.07.017).
- Tapete, D., F. Cigna, and D. N. M. Donoghue. 2016. "Looting Marks' in Space-Borne SAR Imagery: Measuring Rates of Archaeological Looting in Apamea (Syria) with Terrasar-X Staring Spotlight." *Remote Sensing of Environment* 178: 42–58. doi:[10.1016/j.rse.2016.02.055](https://doi.org/10.1016/j.rse.2016.02.055).

- Tapete, D., F. Cigna, N. Masini, and R. Lasaponara. 2013. "Prospection and Monitoring of Thearchaeological Heritage of Nasca, Peru, with ENVISAT ASAR." *Archaeological Prospection* 20: 133–147. doi:[10.1002/arp.v20.2](https://doi.org/10.1002/arp.v20.2).
- Wang, X., J. Lu, H. Yan, and F. Zhao. 2014. "Reports of Archaeological Surveying and Excavation of 2012–2013 in Han Hangu Pass, Xin'an, Henan China." [In Chinese.] *Archaeology* 11: 3–28.